

Supplementary information

A long-persistent phosphorescent chemosensor for the detection of TNP based on $\text{CaTiO}_3:\text{Pr}^{3+}$ @ SiO_2 photoluminescence materials

Fangfang Li^a, Xuan Hu^a, Fengyi Wang^a, Baozhan Zheng^a, Juan Du^{a}, and Dan Xiao^{a, b*}*

^a College of Chemistry, Sichuan University, 29 Wangjiang Road, Chengdu 610064,
PR China.

^b Key Laboratory of Green Chemistry and Technology, Ministry of Education,
College of Chemistry, Sichuan University, Chengdu, Sichuan 610064, China

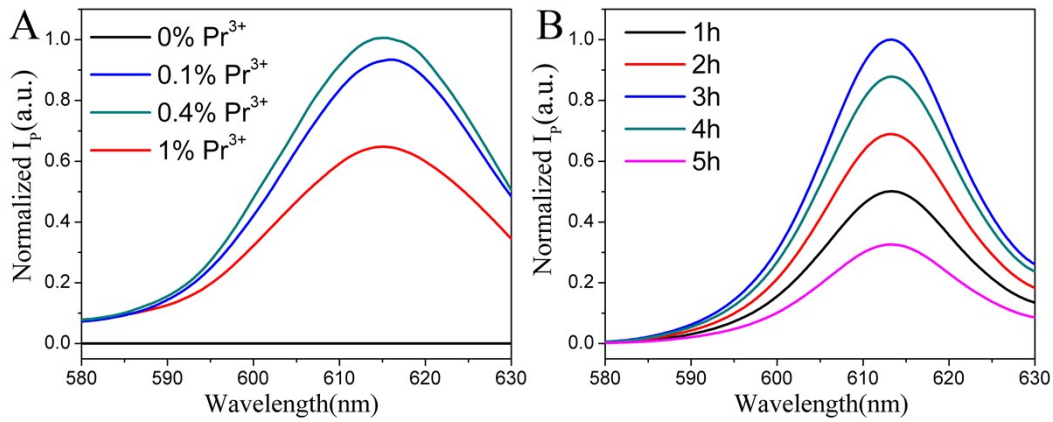


Figure S1. The phosphorescence intensity of (A) different mole ratio of Pr^{3+} doped $\text{CaTiO}_3:\text{Pr}^{3+}$, 900 °C calcination for 3 h. (B) $\text{CaTiO}_3:0.4\%$ Pr^{3+} under different calcination time at 900 °C.

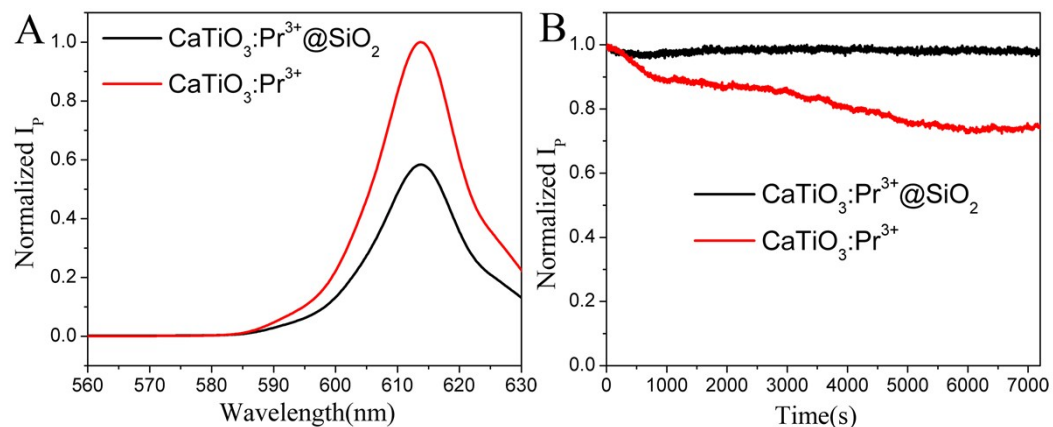


Figure S2. The phosphorescence intensity (A) and the photostability (B) of $\text{CaTiO}_3:\text{Pr}^{3+}$ before and after coated a silica shell in PBS solution (10 mM, pH = 8, $\lambda_{\text{ex}} = 315$ nm).

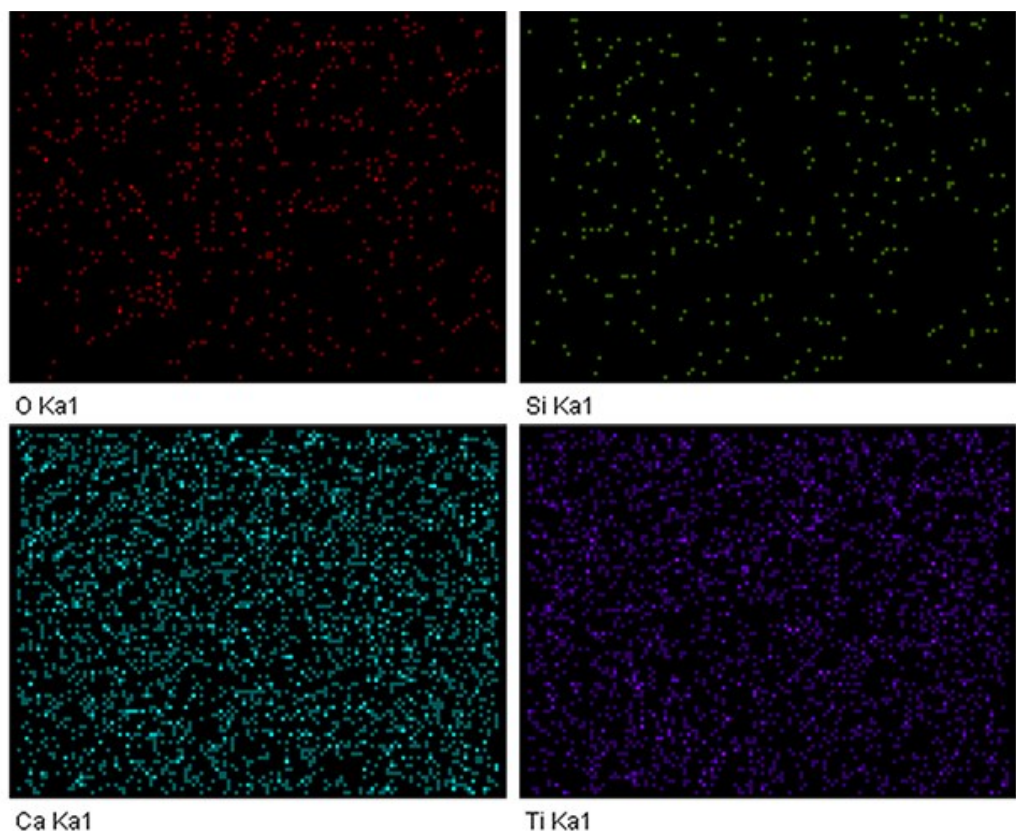


Figure S3. The EDS elemental mapping images of O, Si, Ca and Ti in $\text{CaTiO}_3:\text{Pr}^{3+}@\text{SiO}_2$.

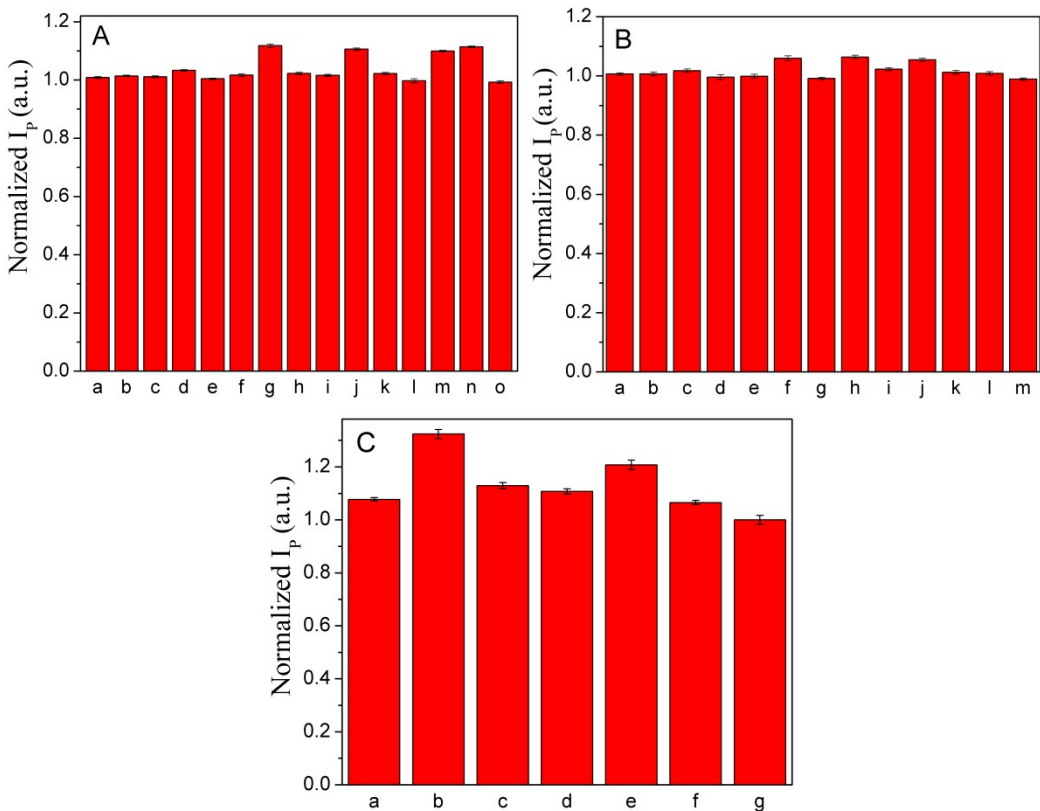


Figure S4. Normalized phosphorescence intensities of $\text{CaTiO}_3:\text{Pr}^{3+}@\text{SiO}_2$ ($30 \mu\text{g/mL}$) to $200 \mu\text{M}$ TNP in the presence of $200 \mu\text{M}$ (A): (a) Na^+ , (b) Mg^{2+} , (c) Al^{3+} , (d) Ca^{2+} , (e) Cr^{3+} , (f) Mn^{2+} , (g) Fe^{3+} , (h) Co^{2+} , (i) Ni^{2+} , (j) Cu^{2+} , (k) Zn^{2+} , (l) Cd^{2+} , (m) Ag^+ , (n) Hg^{2+} , (o) Pb^{2+} . (B): (a) F^- , (b) Cl^- , (c) Br^- , (d) I^- , (e) CO_3^{2-} , (f) oxalate, (g) citrate, (h) NO_3^- , (i) NO_2^- , (j) SO_4^{2-} , (k) SO_3^{2-} , (l) S^{2-} , (m) PO_4^{3-} . (C): (a) Phenol, (b) NT, (c) DNT, (d) TNT, (e) NP, (f) DNP, (g) Blank.

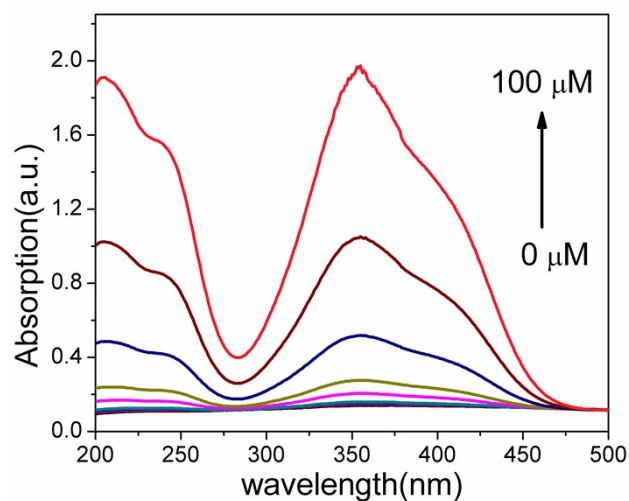


Figure S5. The UV-Vis absorption spectra of $\text{CaTiO}_3:\text{Pr}^{3+}@\text{SiO}_2$ with different concentrations of TNP (0, 0.5, 1, 2, 5, 10, 20, 50 and 100 μM) in 10 mM PBS buffer (pH 8.0).

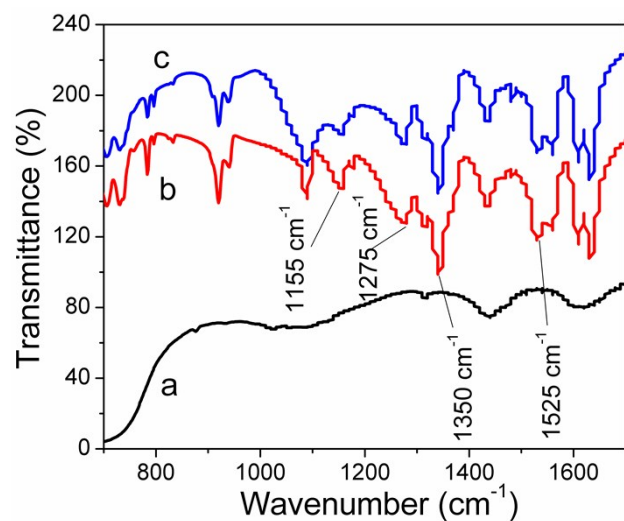


Figure S6. FT-IR spectra of $\text{CaTiO}_3:\text{Pr}^{3+}@\text{SiO}_2$ (a), TNP (b) and $\text{CaTiO}_3:\text{Pr}^{3+}@\text{SiO}_2$ and TNP mixture(c)

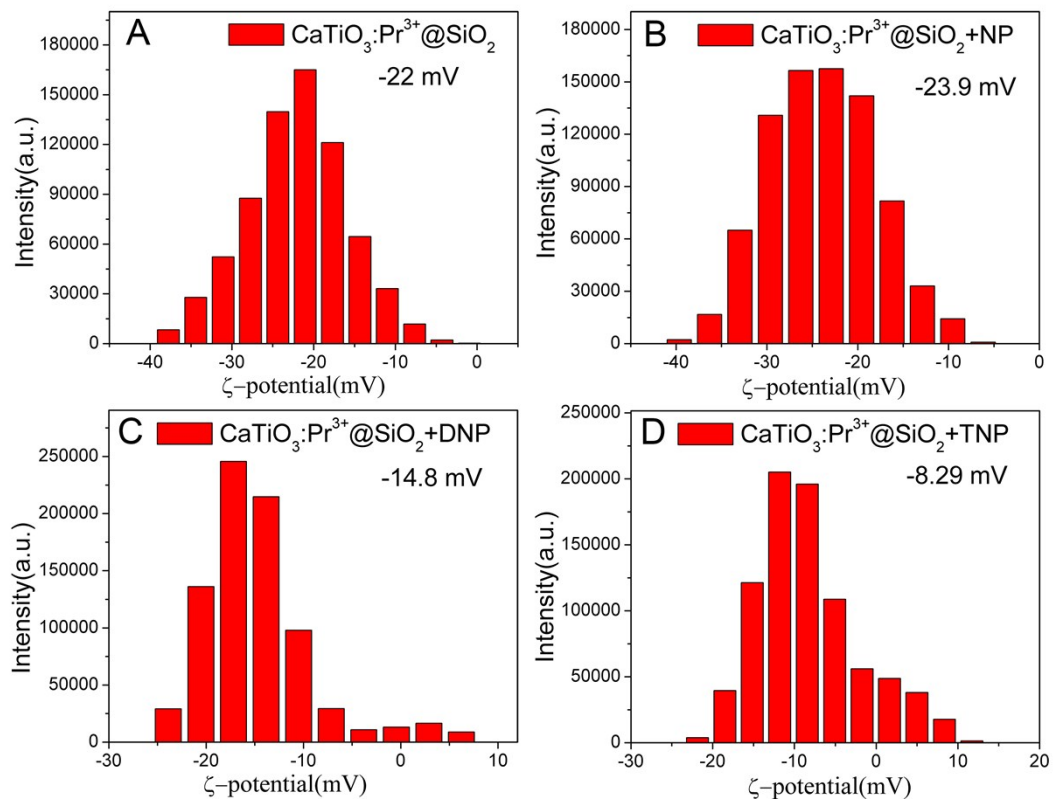


Figure S7. ζ -potential of $\text{CaTiO}_3:\text{Pr}^{3+}@\text{SiO}_2$ (A), and $\text{CaTiO}_3:\text{Pr}^{3+}@\text{SiO}_2$ with NP (B), DNP (C) and TNP (D)

Table S1. Comparison of different system for TNP detection

System	LOD	Linear range	K_{SV}(M⁻¹)	Reference
Molybdenum disulfide (MoS ₂) quantum dots	95 nM	0.099-36.5 μM	4.3×10 ⁴	1
8-Hydroxyquinoline aluminum (Alq3)-based composite nanospheres	32.3 μg/mL (0.141 μM)	0.05-70 μg/mL (0.218-305 μM)	N/A	2
2,6-Diamino pyridine functionalized grapheme oxide (DAP-RGO)	125 nM	N/A	1.322×10 ⁵	3
Ratiometric NIR fluorescent probe DNSA- SQ	70 nM	5-100 μM	N/A	4
1,8-Naphthalimide - anthracene (Nph-An)	0.47 μM	N/A	7.0×10 ⁴	5
Nitrogen doped graphene quantum dots	0.3 μM	1-60 μM	N/A	6
CaTiO ₃ :Pr ³⁺ @SiO ₂ photoluminescence materials	20.6 nM	0.5-100 μM	1.25×10 ⁴	This work

Table S2. Determination of TNP in pond water samples

Samples	TNP		Proposed method		
	Added (μM)	Found (μM)	Recovery (%)	SD (n=3) (μM)	RSD (n=3) (%)
1	20.00	20.32	101.60	0.16	0.79
2	50.00	49.67	99.34	0.07	0.14
3	80.00	80.26	100.33	0.48	0.56

References

- 1 Y. Wang, Y. Ni, *Anal. Chem.*, 2014, **86**, 7463-7470.
- 2 Y. Ma, H. Li, S. Peng, L. Wang, *Anal. Chem.*, 2012, **84**, 8415-8421.
- 3 D. Dinda, A. Gupta, B. K. Shaw, S. Sadhu, S. K. Saha, *Acs Appl. Mater. Inter.*, 2014, **6**, 10722-10728.
- 4 Y. Xu, B. Li, W. Li, J. Zhao, S. Sun, Y. Pang, *Chem. Commun.*, 2013, **49**, 4764-4766.
- 5 H. Ma, C. He, X. Li, O. Ablikim, S. Zhang, M. Zhang, *Sensor. Actuat. B Chem.*, 2016, **230**, 746-752.
- 6 L. Lin, M. Rong, S. Lu, X. Song, Y. Zhong, J. Yan, Y. Wang, X. Chen, *Nanoscale*, 2015, **7**, 1872-1878.